Macromolecules

ARTICLE

pubs.acs.org/Macromolecules

Structure and Rheology of Self-Assembled Telechelic Associative Polymers in Aqueous Solution before and after Photo-Cross-Linking

Vijay Kadam, Taco Nicolai,* Erwan Nicol, and Lazhar Benyahia

Polymères, Colloïdes, Interfaces, UMR-CNRS 6120, Université du Maine, 72085 Le Mans cedex 9, France

ABSTRACT: Poly(ethylene oxide) (PEO) was end-capped with short poly(methacryloyloxyethyl acrylate) (PMEA) chains. In aqueous solutions the end-blocks self-assembled, leading to flower-like polymeric micelles at low concentrations that associated through bridging at higher concentrations. Above a critical percolation concentration (C_p) a system-spanning transient network was formed. The transient self-assemblies were locked-in *in situ* by UV irradiation which caused photo-cross-linking of the PMEA blocks. The structure and composition of the clusters formed at $C < C_p$ was studied by light scattering and chromatography after cross-linking and dilution. The results were compared with mean-field theory and numerical simulations. The dynamic mechanical properties of the networks formed for $C > C_p$ were studied by oscillatory shear before, during, and after irradiation. UV radiation transformed the transient networks into permanent gels within a few seconds.

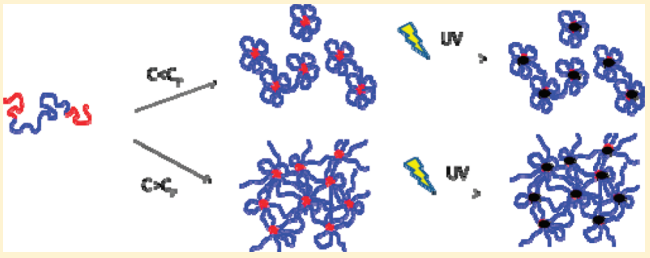

INTRODUCTION

Telechelic associative polymers contain relatively small solvophobic blocks at the chain ends that spontaneously assemble in selective solvents. The structure and the rheology of telechelic polymer solutions have been investigated extensively in the past.[1−3] If only one chain end is functionalized, the chains form star-like polymers above a critical association concentration (cac) in a way analogous to micellization of small surfactants. If both ends are functionalized, the chains either loop back to the same multiplet or form a bridge between two flower-like polymeric micelles leading to aggregation of the micelles. With increasing polymer concentration (C) the micelles associate into more and larger aggregates until at a critical percolation concentration (C_p) a system-spanning network is formed. If the concentration is further increased, an increasing fraction of polymers becomes incorporated into the network.

A consequence of the formation of a transient network is that the viscosity increases strongly with increasing polymer concentration for $C > C_p$. If the lifetime of the bridges is not too short, the shear moduli show elastic behavior at high frequencies and liquid-like behavior at low frequencies. The high-frequency elastic modulus is proportional to the concentration of elastically active chains, but the system can relax at lower frequencies because end-blocks exchange between multiplets. For some systems the relaxation can be described in terms of a single relaxation time, but for others it is characterized by a distribution of relaxation times.

Self-assembly of telechelic polymers can thus be used to create clusters of flower-like polymers, but their structure is dynamic and changes when the concentration or the external conditions are varied. Here we propose a method to fix the self-assembled structures by *in situ* covalent cross-linking of the multiplets. For this purpose we synthesized poly(methacryloyloxyethyl acrylate)-*b*-poly(ethylene oxide)-*b*-poly(methacryloyloxyethyl acrylate (PMEA-*b*-PEO-*b*-PMEA) triblock copolymer. This amphiphilic PEO-based copolymer bears photo-cross-linkable groups on both hydrophobic end-blocks. The same method was used earlier to freeze polymeric micelles formed by PE-based diblock copolymers that were functionalized at one end.[4,5]

Amphiphilic triblock copolymers bearing cross-linkable groups have already been used mainly to synthesize hydrogels for applications in cell encapsulation and tissue engineering.[6] However, we are aware of only one previous investigation of *in situ* photo-cross-linking of self-assembled telechelic polymers that was reported recently by Sanabria-DeLong et al.[7] These authors studied the compression of hydrogels formed after photo-cross-linking poly(lactide)-*b*-poly(ethylene oxide)-*b*-poly(lactide) (PLA-*b*-PEO-*b*-PLA) at relatively high concentrations (>100 g/L). The gels did not show linear response even at very low strain, and various constitutive relationships that can describe the strain−stress behavior were discussed. A different type of systems was investigated by Di Biase et al.[8] They studied Pluronics triblock copolymers with a central insoluble block and two soluble end-blocks. The soluble end-blocks were functionalized and cross-linked *in situ* by irradiation, which may lead to the formation of covalent hydrogels. However, in this case, irradiation does not lock-in existing transient cross-links but creates new cross-links.

Here we investigate self-assembled systems in aqueous solution over a wide range of concentrations (1−120 g/L) before, during, and after irradiation. In this concentration range jamming of the micelles is not yet important. We will show that self-assembled

Received: May 12, 2011
Revised: September 8, 2011
Published: September 26, 2011

Chart 1. Chemical Formula of the Poly(methacryloyloxyethyl acrylate)-*b*-poly(ethylene oxide)-*b*-poly(methacryloyloxyethyl acrylate) (PMEA-*b*-PEO-*b*-PMEA) Triblock Copolymer

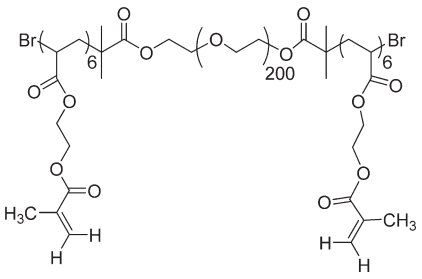

structures formed in aqueous solution can be locked-in very rapidly by using UV-irradiation with modest changes in the structure. The clusters that formed at $C < C_p$ were studied using light scattering and size exclusion chromatography (SEC), and the gels formed at $C > C_p$ were characterized using rheometry. The results will be compared with mean-field theory and recent numerical simulations of reversibly aggregating spheres.[9]

EXPERIMENTAL SECTION

Materials. *Synthesis of PMEA$_6$-b-PEO$_{200}$-b-PMEA$_6$ Triblock Copolymer (Chart 1).* The methacrylate-functionalized triblock copolymer was synthesized by atom transfer radical polymerization (ATRP) according to a procedure described elsewhere.[5] The number (M_n) and weight (M_w) averaged molar mass of the polymers were determined using size exclusion chromatography (SEC), light scattering (LS), and ^{1}H NMR: $M_{n,NMR}(CDCl_3) = 12.8 \times 10^3$ g mol^{-1}, $M_{n,SEC}(THF) = 11.5 \times 10^3$ g mol^{-1}, $M_{w,SEC}(THF) = 12.4 \times 10^3$ g mol^{-1}, $M_{w,LS}$(acetonitrile) = 13.3×10^3 g mol^{-1}. THF and acetonitrile are good solvents for both blocks. The degree of polymerization of each PMEA block was found to be 6 from ^{1}H NMR measurements. SEC showed that about 9% w/w of the polymers was linked to another polymer during the last synthesis step as this population had exactly twice the molar mass of the main population (ABAABA). When these polymers associate, they form two loops or bridges per chain with the same length as the other chains.

Photo-Cross-Linking. For photo-cross-linking experiments a solution of 2,2-dimethoxy-2-phenylacetophenone (DMPA) photoinitiator (0.01 M) was prepared in THF. The molar ratio of DMPA to polymer was fixed at 0.17, which corresponds to on average about 3 molecules per micelle considering that the number average number of hydrophobic blocks per multiplet is 31 (see Results and Discussion). The required amount of solution of DMPA was placed on the walls of a glass vial, and THF was evaporated off under a gentle flow of argon, after which the polymer dissolved in deionized Milli-Q water was introduced into the vial that was sealed with a rubber septum. The vial was rotated overnight on a roller stirrer. Just before the photo-cross-linking experiment, the solution was bubbled by purging argon for 15 min to remove traces of dissolved oxygen. At concentrations below C_p the samples were photo-cross-linked in a glass vial by irradiation for 60 s with UV light at 365 nm with an intensity of 0.4 W cm^{-2}. At higher concentrations the samples were photo-cross-linked after loading into the rheometer (see below). All samples were transparent and homogeneous both before and after irradiation.

Methods. *Size exclusion chromatography (SEC)* in THF was done with a system consisting of a Spectra System AS100 autosampler and a column (Jordi gel pore size: 500 Å, particle size: 5 μm, length 50 cm) followed by a Spectra Physics RI-71 refractive index detector and a Spectra Physics UV detector (λ = 254 nm). The flow rate of the eluent was 1 mL min^{-1}. The column was calibrated with PEO standards. The experiments were done at 20 °C in an air conditioned room.

SEC in DMF containing 0.01 M LiBr was done on a system consisting of a Waters 510 pump, with a Guard column (Polymer Laboratories, PL gel 5 μm Guard column, 50 × 7.5 mm) followed by two columns (Polymer Laboratories (PL), 2 PL gel 5 μm Mixed-D columns, 300 × 7.5 mm), with a Waters 410 RI detector. The flow rate of eluent was 1 mL min^{-1} at 30 °C. Polystyrene standards were used for calibration. DMF is a good solvent for both blocks, and the addition of 0.01 M LiBr results in an efficient separation of the cross-linked micelles that were prepared in water. The solvent was subsequently exchanged to DMF for SEC analysis using a rotary evaporator. Of course, the solvent exchange does not modify the structure of the micelles after cross-linking.

Fluorescence spectra were recorded with a Horiba-Jobin Yvon fluorescence spectrophotometer in the right-angle geometry. For the fluorescence measurements, 3 mL of each sample was placed in a 1 cm square quartz cell. The emission spectra were recorded using the excitation wavelength at 329 nm, and the excitation spectra were recorded using the emission wavelength at 371 nm. The slit widths were set at 2 nm for both excitation and emission fluorescent measurements.

Samples were prepared as follows. 18 μL of a pyrene solution in THF (10^{-4} M) was placed on the wall of a glass vial and rotated under gentle flow of N_2 to evaporate the THF and to form a film of pyrene. Aqueous polymer solutions were prepared in deionized Milli-Q water by diluting stock solutions to the desired polymer concentration (from 1×10^{-4} to 10 g L^{-1}). 3 mL of polymer solution was added to the vial to yield a final pyrene concentration of 6×10^{-7} M for each sample. The pyrene containing samples were stirred for 2 days in the dark at room temperature.

Light scattering measurements were done using commercial static and dynamic light scattering equipment (ALV-Langen, Germany) equipped with an He−Ne laser emitting vertically polarized light at λ = 632 nm. The temperature was set at 20 °C and controlled by a thermostat bath to within ±0.1 °C. Measurements were made at scattering angles (θ) between 12° and 150°.

In static light scattering experiments the relative excess scattering intensity (I_r) was determined as the total intensity minus the solvent scattering divided by the scattering of toluene at 20 °C. In dilute solutions I_r is related to the weight average molar mass (M_w) and the z-average structure factor ($S(q)$):[10,11]

$$I_r = KCM_wS(q) \quad (1)$$

with C the solute concentration and K an optical constant that depends on the refractive index increment. $S(q)$ describes the dependence of I_r on the scattering wave vector: $q = (4\pi n/\lambda)\sin(\theta/2)$. At higher concentrations interactions influence the scattering intensity, and the result obtained by extrapolation to $q = 0$ is only an apparent molar mass (M_a).

In dynamic light scattering measurements the normalized electric field autocorrelation function ($g_1(t)$) was calculated from the measured intensity correlation function ($g_2(t)$) using the so-called Siegert relation.[12] $g_1(t)$ was analyzed in terms of a relaxation time distribution using the REPES routine.[13,14] The average relaxation rate (Γ) was found to be q^2-dependent, and a diffusion coefficient (D) was calculated as $D = \Gamma/q^2$. At sufficiently low concentrations, where interaction is negligible, the z-average hydrodynamic radius (R_h) of the solute can be calculated from the diffusion coefficient using the Stokes−Einstein relation:

$$R_h = \frac{kT}{6\pi\eta D} \quad (2)$$

with η the solvent viscosity, k Boltzmann's constant, and T the absolute temperature. At higher concentrations an apparent hydrodynamic radius (R_{ha}) is obtained in this manner.

Rheology. The rheological measurements were done at 20 °C with stress-controlled rheometers (ARG2 (Rheometrics) and MCR-301

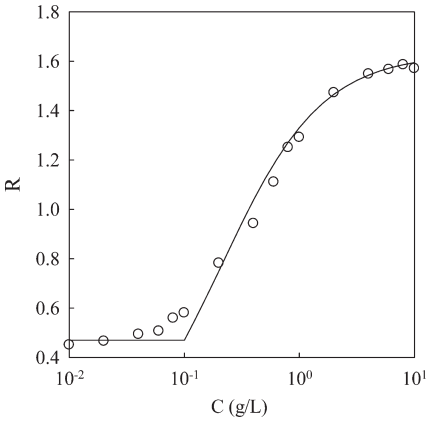

Figure 1. Ratio of the fluorescence intensities at 337.6 and 333.8 nm from pyrene excitation spectra as a function of the $PMEA_6$-*b*-PEO_{200}-*b*-$PMEA_6$ concentration. The solid line represents a fit to eq 3; see text.

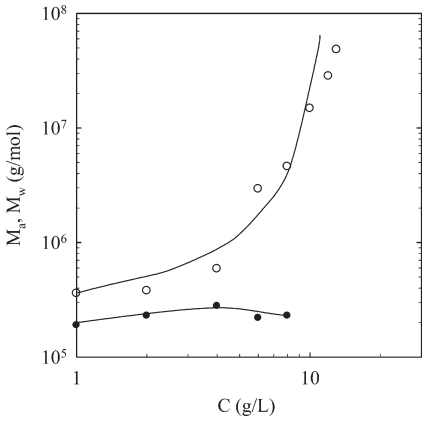

Figure 2. Dependence on the concentration at which the systems were cross-linked of the apparent molar mass of aqueous solutions of $PMEA_6$-*b*-PEO_{200}-*b*-$PMEA_6$ before irradiation determined *in situ* (filled symbols) and the weight average molar mass obtained after *in situ* UV-irradiation determined after dilution in water (open circles). The line through the open points corresponds to results from computer simulations, see explanation after eq 4, while the line through the filled points is a guide to the eye.

(Anton Paar)) using cone and plate geometries. The measurements were done in the linear response regime except when it is explicitly stated that we study nonlinear rheology. For *in situ* photo-cross-linking, the samples were introduced into the geometry under a gentle flow of argon, and the sample was covered with mineral oil in order to avoid evaporation. The flow of argon was stopped just before the start of the experiment. A UV light guide from Dymax Bluewave-200 spot-curing equipment (wavelength = 365 nm) was positioned 5 cm below the glass plate. The samples were irradiated at 0.17 W cm^{-2} for durations between 5 and 90 s. The temperature increase during irradiation was less than 5 °C.

RESULTS AND DISCUSSION

Fluorescence Spectroscopy. The onset of formation of the micelles in aqueous solution was evaluated using steady-state fluorescence of pyrene.[15,16] The small fraction (9%) of longer chains formed during the synthesis are expected to have a slightly lower cmc, but the effect on the measurements will be very small. The dependence on the polymer concentration of the intensity ratio of the pyrene excitation bands at 337.6 and 333.8 nm (R) is shown in Figure 1. As demonstrated by Wilhelm et al.,[15] the ratio of the amount of pyrene per unit of volume situated in the micellar cores $[Py]_m$ to that in the aqueous phase $[Py]_w$ is given by

$$\frac{[Py]_m}{[Py]_w} = \frac{R - R_{min}}{R_{max} - R} = \frac{K\chi_{PMEA}(C - cmc)}{1000\rho_{PMEA}} \quad (3)$$

where K is the partition coefficient of pyrene between the aqueous and micellar phase, χ_{PMEA} is the weight fraction of the PMEA block in the copolymer, and ρ_{PMEA} is the density of the PMEA.

Except close to C = cmc, the experimental results can be well described using eq 3 with cmc = 0.1 g L^{-1} and $K = 1.7 \times 10^4$. The value of χ_{PMEA} = 0.17 was calculated from the experimentally determined average composition of the polymers, and ρ_{PMEA}= 1.1 g/mL was approximated by the value of pure poly(alkyl acrylate) taken from the literature. We note that the quality of the fit is not very sensitive to the exact value of cmc. From the light scattering results shown below (Figure 2) we estimated that the molecular weight of the micelles is about 2.0×10^5 g mol^{-1}. This means that when $[Py]_m$ is equal to $[Py]_w$, about one in five micelles contains a pyrene molecule.

Characterization of the Clusters. Static and dynamic light scattering measurements were done on aqueous polymer solutions before and after cross-linking. For systems that were investigated the q dependence was very small so that no information could be obtained about the structure. As explained in the Experimental Section, M_w and R_h of the micelles can be determined in very dilute solutions maintaining $C \gg$ cmc. With increasing concentration the micelles increasingly associate by forming bridges leading to an increase of M_w and R_{hz}. At higher concentrations we also have to consider the excluded volume interactions between the micelles, which cause a decrease of the apparent molar mass (M_a) and hydrodynamic radius (R_{ha}). Therefore, with increasing polymer concentration M_a and R_{ha} are expected to increase first because association initially dominates compared to repulsive interactions and then decreases when repulsive interactions become preponderant. This behavior was shown in more detail elsewhere for the same PEO chains end-capped with alkyl groups.[17]

For the present system we determined M_a and R_{ha} before irradiation over a limited range of concentrations between 1 and 8 g L^{-1} because at higher concentrations it was difficult to filter the solutions through 0.2 μm filters and a small fraction of large aggregates perturbed the measurements. The concentration dependence of M_a in this range is very weak, which means that interactions largely compensate the effect of association (see Figure 2). R_{ha} remained about 13 nm in this concentration range.

In order to determine the true molar mass of the micelles, one needs to extrapolate to low concentrations where interactions can be neglected while keeping $C \gg$ cmc. For the system studied here cmc $\approx$ 0.1 g L^{-1}, which means that the effect of the cmc cannot be ignored at C = 1 g L^{-1}. SEC experiments discussed below show that at 1 g L^{-1} about 10% of the chains does not associate and about 12% of the micelles forms dimers. Thus, the effects of the cmc and the formation of dimers compensate each other at this concentration, which means that M_a at 1 g L^{-1} is not far from the true molar mass of the micelles if we may ignore the effect of interactions: $M_{mic} \approx 2.0 \times 10^5$ g/mol. Therefore, we estimate that the aggregation number, i.e., the number of associated PMEA groups per micelle, is about 31, though this may be an underestimate because we neglect excluded volume interactions. The values of the aggregation number and the hydrodynamic radius are comparable to those observed for polymeric

micelles formed by the same PEO chains end-capped at both ends with octadecyl[17] and for micelles formed by PEO chains with half the molar mass end-capped at one end with octadecyl[17] or with a poly(ethyl acrylate) (PEA) decamer.[18]

The self-assembled systems were subsequently locked-in by cross-linking the multiplets by UV-irradiation. After cross-linking, the systems could be diluted without modifying their structure. In this way M_w and R_{hz} of the aggregates formed by bridging of multiplets could be determined without the influence of interactions. For the measurements the solutions were highly diluted, and it was verified that further dilution had no effect on the measured values of M_w and R_{hz}. Figure 2 shows that M_w increased with increasing concentration starting at a value (M_{mic} = 3.6×10^5 g/mol at C = 1 g/L) that is significantly larger than that obtained before cross-linking even considering the effect of exclude volume interactions in the latter case. In the calculation of M_{mic} we considered the fraction of dimers and free chains obtained from SEC (see below). The implication is that the average aggregation number is increased during cross-linking to about 56. The value of R_{hz} at 1 and 2 g/L remained approximately the same after cross-linking, which is not surprising considering the very weak dependence of R_h on the aggregation number. If the exchange of individual chains is rapid compared to the initiation of the cross-linking process, it may lead an increase of the molar mass of the micelles during the cross-linking process. However, recently, an investigation was reported of PEO chains with half the molar mass used here and functionalized at one end by a poly(ethyl acrylate) block bearing cross-linkable methacrylate functions.[5] It was found that for that system M_{mic} and R_{hz} were close to those found here and did not change significantly after UV-induced cross-linking.

M_w of the cross-linked samples increased sharply between 10 and 13 g L^{-1}, and at higher concentrations the system no longer fully dispersed when diluted, indicating that a gel had been formed. The large difference between M_a and M_w illustrates well the dominant effect of interactions and thus the need to covalently fix and dilute the systems in order to characterize them properly. If the structure is not modified by the cross-linking, the *in situ* scattering intensity should remain the same after cross-linking. Here we observed a systematic increase of the intensity by almost a factor of 2 probably due to the increase of the size of the micelles.

M_w of the cross-linked samples is plotted in Figure 3 as a function of R_{hz} and is compatible with a power law: $M_w \propto R_{hz}^2$. The exponent in this relation is the so-called fractal dimension d_f of the particles. A fractal dimension of about two is not a unique feature as it is predicted for different structures such as flexible linear chains and random aggregates. In the context of the present study, we point out that d_f = 2.0 is also theoretically predicted for large clusters of particles if all configurations have the same probability, which is the case for dilute reversibly associated particles at equilibrium.[19,20] On the other hand, numerical simulations show that at concentrations very close to the percolation threshold the clusters should have a fractal dimension of 2.5.[9] However, in this case the clusters are extremely polydisperse, which causes a reduction of the measured apparent fractal dimension to d_f = 2.0.[21] Therefore, theoretically in both regimes an exponent of 2.0 is predicted, and this value is thus expected also at the intermediate concentrations at which the experiments were done.

In order to obtain more detailed information about the size distribution, we analyzed the samples with SEC in DMF (see Figure 4a). The chromatographs of un-cross-linked systems show two distinct peaks corresponding to unimers and a small

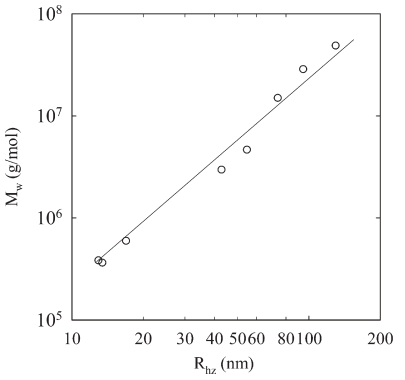

Figure 3. Double-logarithmic representation of M_w vs R_{hz} of the clusters obtained after *in situ* UV-irradiation of aqueous solutions of $PMEA_6$-*b*-PEO_{200}-*b*-$PMEA_6$ at different concentrations and measured after dilution in water (circles). The solid line has a slope of 2.

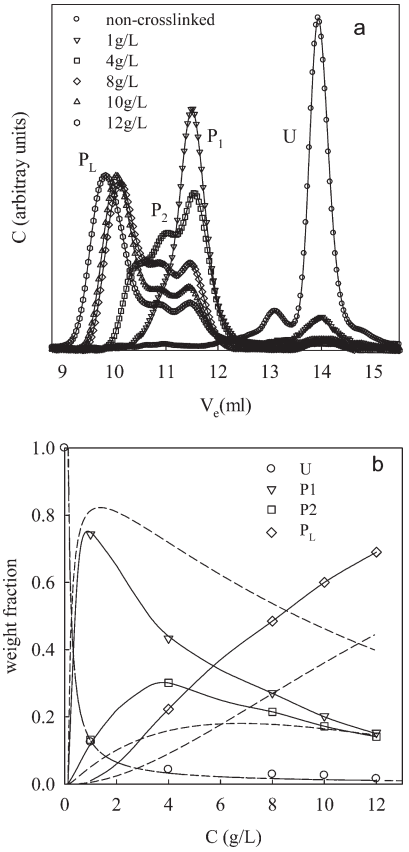

Figure 4. (a) Chromatograms obtained by SEC in DMF of $PMEA_6$-*b*-PEO_{200}-*b*-$PMEA_6$ after *in situ* irradiation at different concentrations in aqueous solutions. (b) Weight fractions of the unimers (U), individual micelles (P_1), dimers of micelles (P_2), and larger micelle clusters (P_L) as a function of the polymer concentration at which the samples were irradiated. The dashed lines represent calculated values as explained in the text, and the solid lines are guides to the eye.

fraction of end-linked chains with twice the molar mass. After cross-linking at different concentrations we observe in addition to the weight fraction of residual unassociated chains (U) three peaks corresponding to the weight fractions of single micelles (P_1),

micelle dimers (P_2), and larger micelle clusters (P_L). The relative amplitudes of each peak, shown in Figure 4b, correspond to the weight fractions of each population. With increasing concentration P_1 increases first rapidly for $C >$ cmc as micelles are being formed and then decreases as more micelles become cross-linked. P_2 increases first as more micelles bridge to form dimers but decreases again at higher concentrations when more dimers are connected into larger clusters. P_L increases progressively with increasing concentration.

U was about 0.1 at $C = 1$ g L^{-1} and decreased rapidly with increasing concentration. For an ideal micellization process $U =$ cmc/C. A good description of the data could be obtained assuming cmc = 0.13 g L^{-1} (see dashed line through the data in Figure 4b), which is compatible with the fluorescence results shown above. This means that irradiation does not modify strongly the fraction of free unimers.

If it is true that the irradiated system represents the equilibrium state of the self-assembled polymers, we may compare the experimental results with theoretical predictions for reversibly aggregating particles. When interpreting the results, we will ignore in the presence of a small fraction of chains with twice the molar mass of the central block in the experimental system. These chains are not expected to show very different association behavior but may influence weakly the average aggregation number of the micelle. The effect on the cluster size distribution and the rheology is expected to be small. The equilibrium cluster size distribution can be calculated analytically if it is assumed that all bonds are equi-probable.[22] Considering that the micelles can form up to 56 bonds, we can use the limit of large functionality of this mean-field theory. The molar concentration of clusters containing n micelles ($X(n)$) at a given total micelle concentration (X_0) depends on the bond energy but can also be described in terms of the micelle concentration at the percolation threshold (X_p):

$$\frac{X(n)}{X_p} = \left[\frac{X_0}{X_p}\exp\left(-\frac{X_0}{X_p}\right)\right]^n \frac{n^{n-2}}{n!} \quad (4)$$

Here $X_0 = (C - \text{cmc})/M_{mic}$ and $X_p = (C_p - \text{cmc})/M_{mic}$. The weight fraction of monomers ($n = 1$) and dimers ($n = 2$) is given by $P_n = nX(n)M_{mic}/C$. The weight fraction of all clusters with $n > 2$ is given by $P_L = 1 - U - P_1 - P_2$. Notice that when expressed in terms of C_p the calculated values do not depend on M_{mic}. Light scattering and rheology (see below) showed that experimentally C_p is situated between 13 and 14 g L^{-1}. The values calculated from eq 4 with $C_p = 13$ g L^{-1} are compared to the experimental values in Figure 4b. Clearly, mean-field theory underestimates the degree of aggregation. Better, but still not perfect, agreement can be obtained if C_p is chosen to be about 8 g L^{-1}, but this value is not compatible with the experiments.

The situation has also been investigated using numerical simulations.[9] In these simulations, mondisperse spheres are moved randomly with very small steps. The spheres are not allowed to overlap and bind with a set probability when they are within a set distance from each other. Bound particles move cooperatively leading to Brownian motion with a diffusion coefficient inversely proportional to the radius of the aggregates. Reversibility is simulated by letting bonds break with a set probability. Bond breaking and formation leads to an effective attractive interaction that can be expressed in terms of a second virial coefficient (B_2). The simulations have shown that the equilibrium state for reversibly aggregating spheres with a narrow interaction range is determined by B_2 independent of the interaction range. B_2 is the sum

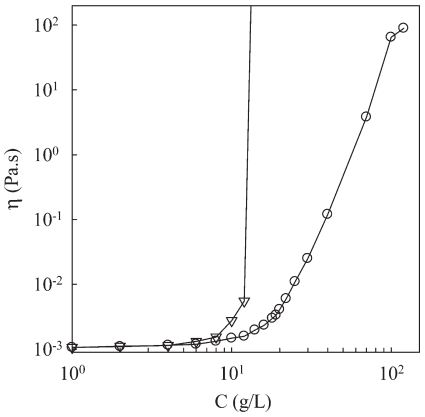

Figure 5. Concentration dependence of the viscosity of aqueous solutions of PMEA$_6$-*b*-PEO$_{200}$-*b*-PMEA$_6$ before (circles) and after (triangles) irradiation. The viscosity was measured in the linear response regime.

of the excluded volume repulsion and the square-well attraction: $B_2 = B_{rep} - B_{att}$. Expressed in units of the particle volume $B_{rep} = 4$. The value of B_{att} in the same units can be obtained experimentally from the fraction of dimers at low concentrations:

$$N(2)/N_{tot} = B_{att}\varphi \quad (5)$$

where $\varphi = N_{tot}N_a 4\pi R_h^3/3$ is the volume fraction of the spheres with N_a Avogadro's number and $N_{tot} = (C - \text{cmc})/M_{mic}$. B_{att} can thus be calculated from the value of $P_2 = 0.132$ at $C = 1$ g/L using $P_2 = 2N(2)M_{mic}/C$ if we know R_h and M_{mic}. The values of B_{att} and φ are sensitive to small variations of M_{mic} and especially R_h. Using $M_{mic} = 3.6 \times 10^5$ g/mol and $R_h = 13$ nm, we find $B_{att} = 5.7$ and $B_2 = -1.7$ if we assume $B_{rep} = 4$.

In the simulations the system percolates at $\varphi_p = 0.15$ for this value of B_2 almost independently of the width of the interaction range at least if it is less than half of the particle radius.[9] It will be shown below that experimentally we find that C_p is situated between 13 and 14 g L^{-1}, i.e., $\varphi_p \approx 0.2$ using $M_{mic} = 3.6 \times 10^5$ g/mol and $R_h = 13$ nm. The simulations showed that for small volume fractions ($\varphi < 0.15$) M_w was approximately the same for a given value of $B_2\varphi$. This allows us to compare the experimental dependence of M_w on C with that found in the simulations. Qualitative agreement was found using $M_{mic} = 3.6 \times 10^5$ g/mol and $R_h =$ 13 nm (see Figure 2). The comparison shows that the self-assembly of polymeric micelles is indeed a process of random reversible aggregation that is reasonably well described by the computer simulations in which the micelles are considered as hard spheres with short-range attraction.

Rheology. Figure 5 shows the concentration dependence of the zero-shear viscosity at 20 °C of the aqueous polymer solutions before and after cross-linking. For un-cross-linked samples we observed a strong but continuous increase of η (for $C >$ 15 g L^{-1}), which is typical of a transient network. The viscosity of cross-linked samples started to increase at somewhat lower concentrations and diverged at 14 g L^{-1}, where a very weak covalently cross-linked gel was formed. The percolation concentration of this system is thus situated between 13 and 14 g L^{-1}.

The frequency dependence of the shear moduli was determined as a function of temperature for $C = 120$ g L^{-1} before cross-linking. A master curve could be constructed by time–temperature superposition (see Figure 6). From the shift factors we obtained an activation energy of 65 kJ mol^{-1}. The relaxation of the transient network is characterized by a broad distribution

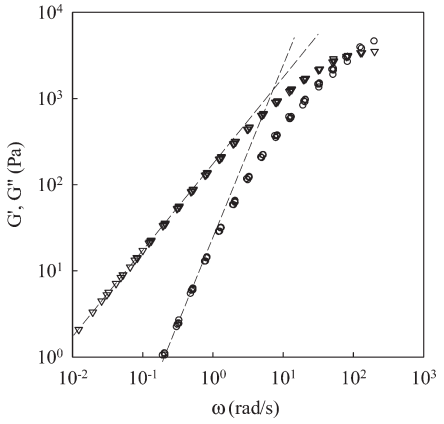

Figure 6. Master curves of the frequency dependence of the shear moduli of an aqueous solution of $PMEA_6$-*b*-PEO_{200}-*b*-$PMEA_6$ at C = 120 g L^{-1} before cross-linking. The master curve at reference temperature 20 °C was obtained by time−temperature superposition of results obtained between 5 and 30 °C. The dashed lines represent the limiting behavior for liquids: $G' \propto \omega^2$ and $G'' \propto \omega^1$.

of relaxation times so that the master curve cannot be described by the Maxwell equation. The terminal relaxation time can be roughly estimated as 0.2 s at 20 °C from the crossing point of the dashed lines, which describe the terminal frequency dependence of storage G' and loss G'' shear moduli. We note that the molar mass of the PEO chains is too small for entanglements to have a significant effect in the concentration range covered here.

The process of freezing-in the transient network by photo-cross-linking was investigated by irradiating the system for 90 s while measuring the shear moduli at a frequency of 1 Hz. The evolution of G' is shown in Figure 7a for a range of polymer concentrations. Except close to C_p, G' increased sharply as soon as the sample was irradiated. After the initial sharp increase, G' continued to increase more slowly until irradiation was stopped and then it decreased slightly. The slow increase of G' is better seen at lower concentrations where the gels are weaker.

Close to C_p, G' did not increase immediately upon irradiation, but only after a lag time that increased with decreasing concentration and that was much longer than the irradiation time for $C <$ 20 g L^{-1}. Notice that also at slightly higher concentrations a very slow increase of G' can be seen long after irradiation has stopped. Currently, we can only speculate that this behavior might be caused by trapped active radicals that slowly cross-link chains that were not yet cross-linked during irradiation.

The frequency dependence of G' and G'' of the systems after irradiation showed that G' was independent of the frequency and orders of magnitude larger than G''. The concentration dependence of the gel modulus (G_0) is plotted as a function of the concentration in Figure 7b. G' increased sharply at $C_p \approx 14$ g L^{-1} followed by a weaker increase at higher concentrations. If the origin of the elastic modulus is rubber elasticity, then G_0 is proportional to the molar concentration of elastically active chains (ν): $G_0 \approx \nu RT$. If all chains are elastically active, then $\nu = C/M_n$. The dashed line represents CRT/M_n and shows that at high concentrations G_0 is somewhat larger, indicating that there is an additional contribution to the elastic modulus at the highest concentrations. The value of G_0 at 120 g L^{-1} may be compared to that of the transient network before cross-linking that can be estimated from G' at high frequencies. Even though G' is still significantly smaller than G_0 at the highest frequency at which it

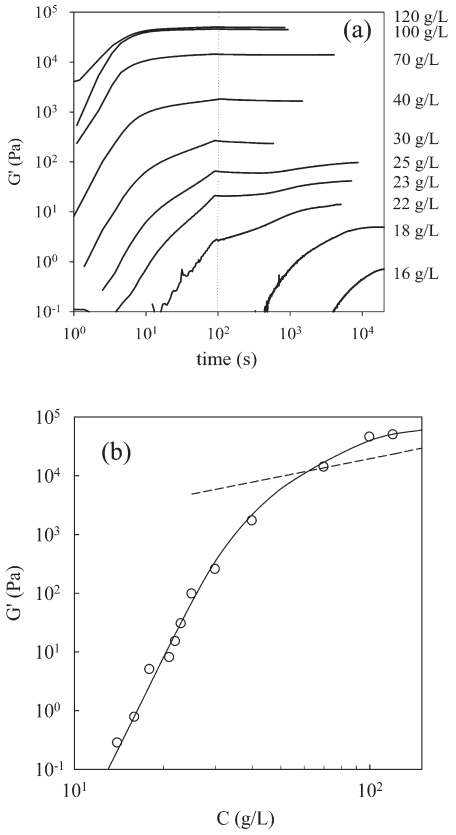

Figure 7. (a) Time dependence of G' at 1 Hz after turning on the UV-lamp for aqueous solutions of $PMEA_6$-*b*-PEO_{200}-*b*-$PMEA_6$ at different concentrations. The dashed line indicates when the lamp was turned off. (b) Concentration dependence of G' for gels formed by irradiating aqueous solutions of $PMEA_6$-*b*-PEO_{200}-*b*-$PMEA_6$. The dashed line represents $G' = CRT/M_n$, while the solid line is a guide to the eye.

could be determined, extrapolation to higher frequencies would give a value that is compatible with G_0. This suggests that UV-irradiation basically locks-in the existing transient network, although some moderate changes cannot be ruled out as judged from the effect of irradiation for dilute micelles.

Compared to the strong concentration dependence, the shear modulus depended little on the duration of the irradiation (see Figure 8a), and even irradiation times as short as 5 s were enough to form gels rapidly at least at concentrations not too close to C_p. However, G' showed subtle effects that are better seen on a linear scale (see Figure 8b). When the irradiation time was 90 s, G' relaxed just after turning off the UV-lamp before increasing again at longer times. The relaxation was still visible for smaller irradiation times, but it was dominated by the increase. Repeated irradiations on cross-linked gels showed in each case a weak relatively slow increase during irradiation followed by relaxation after the lamp was turned off (results not shown). We have verified that the temperature increase of the sample during irradiation is less than 5 °C. We speculate that irradiation leads to tension in the network, which slowly relaxes to steady state after irradiation has stopped. Unfortunately, we do not know the origin of this curious behavior.

The effect of the oscillation amplitude (γ) on the shear modulus of the gels is shown in Figure 9. At low concentrations we observed significant shear hardening of the bridging chains starting at $\gamma \approx$ 50% followed by a sudden drop due to fracture. The shear hardening is possibly due to non-Gaussian stretching[23] even though the chains

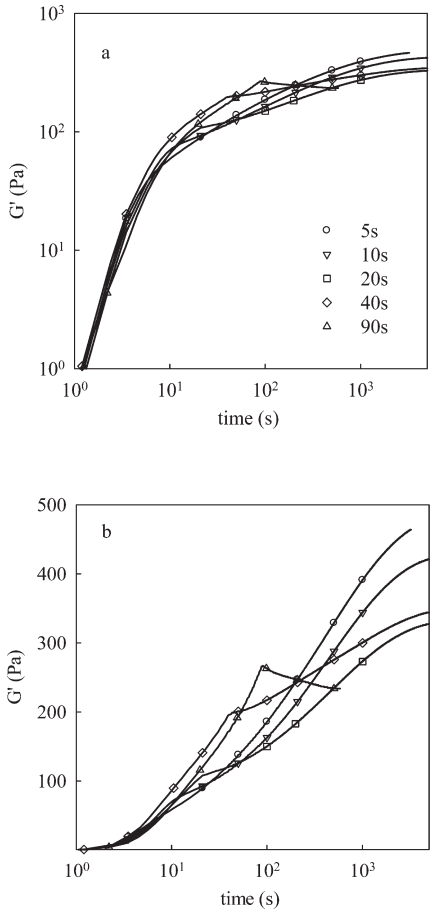

Figure 8. Log−log (a) and lin−log (b) representation of the time dependence of G' at 1 Hz of an aqueous solutions of $PMEA_6$-*b*-PEO_{200}-*b*-$PMEA_6$ at C = 30 g/L after turning on the UV-lamp for different durations indicated in the figure.

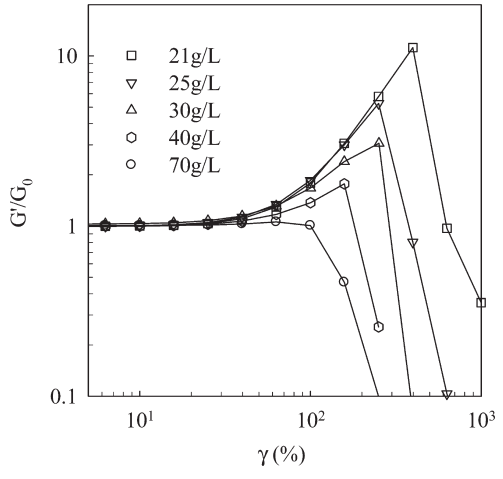

Figure 9. Storage shear modulus at f = 1 Hz normalized by G_0 as a function of the maximum deformation during oscillation for gels formed by irradiating aqueous solutions of $PMEA_6$-*b*-PEO_{200}-*b*-$PMEA_6$ at different concentrations indicated in the figure.

are still only weakly stretched at $\gamma \approx 50\%$. The relative amplitude of shear hardening decreased with increasing concentration, and it was no longer observed at $C = 70$ g L^{-1} or higher. If we consider that G_0 is proportional to the number of elastic strands, then Figure 9 shows how the fracture stress per elastic chain decreases with increasing C. However, in this range the shear modulus increased by more than 3 orders of magnitude, which means that the absolute fracture stress of these gels increased very strongly with increasing polymer concentration from about 10 Pa at 18 g L^{-1} to about 10^3 Pa at 70 g L^{-1}. The critical deformation of fracture decreased relatively weakly from about 400% at C = 18 g L^{-1} to about 100% at C = 70 g L^{-1}.

CONCLUSIONS

PEO chains that are end-capped with short hydrophobic blocks associate into spherical aggregates in a manner analogous to micellization of molecular surfactants. When the chains are end-capped at both ends, the micelles can bridge leading to the formation of larger clusters or a transient gel. By introducing photo-cross-linkable units into the hydrophobic blocks, the transient structure of self-assembled telechelic polymers in aqueous solution can be rapidly locked-in by UV-irradiation with moderate changes to the structure. This allows one to analyze the composition and structure of the clusters formed as a function of the concentration below the percolation threshold. This cannot be done without *in situ* cross-linking because it is necessary to dilute the samples to remove the effect of interactions without restructuring. The aggregate size distribution is not accurately predicted by a mean-field approach. However, comparison with numerical simulations shows that self-assembly of polymeric micelles can be well described as reversibly aggregating hard spheres with short-range attraction.

The transient network that is formed by the telechelic polymers above the percolation threshold can be quickly transformed into a covalently bonded gel by UV-irradiation. The elastic modulus of the gels increases rapidly with increasing concentration and until it becomes comparable to that predicted for an ideal rubbery network for concentrations larger than about 5 times the percolation threshold. With increasing deformation, weak gels formed at lower concentrations show shear hardening before fracture. The relative amplitude of the shear hardening decreases with increasing concentration and only fracture is seen for strong gels.

AUTHOR INFORMATION

Corresponding Author

*E-mail: taco.nicolai@univ-lemans.fr.

ACKNOWLEDGMENT

The authors thank the National Research Agency (ANR program HYPARC) for their financial support. Sagrario Pascual and Hien The Ho are acknowledged for SEC analyses in DMF.

REFERENCES

(1) Winnik, M. A.; Yekta, A. Associative polymers in aqueous solution. *Curr. Opin. Colloid Interface Sci.* **1997**, *2*, 424–36.

(2) Hamley, I. W. *Block Copolymers in Solution*; Wiley: Chichester, 2005.

(3) Chassenieux, C.; Nicolai, T.; Benyahia, L. Rheology of associative polymer solutions. *Curr. Opin. Colloid Interface Sci.* **2011**, *16*, 18–26.

(4) Nicol, E.; Niepceron, F.; Bonnans-Plaisance, C.; Durand, D. Nanostructures from photo-cross-linked amphiphilic poly(ethylene oxyde)-b-alkyl diblock copolymers. *Polymer* **2005**, *46*, 2020–2028.

(5) Piogé, S.; Nesterenko, A.; Brotons, G.; Pascual, S.; Fontaine, L.; Gaillard, C. d.; Nicol, E. Core Cross-Linking of Dynamic Diblock Copolymer Micelles: Quantitative Study of Photopolymerization Efficiency and Micelle Structure. *Macromolecules* **2011**, *44* (3), 594–603.
(6) Nuttelman, C. R.; Rice, M. A.; Rydholm, A. E.; Salinas, C. N.; Shah, D. N.; Anseth, K. S. Macromolecular monomers for the synthesis of hydrogel niches and their application in cell encapsulation and tissue engineering. *Prog. Polym. Sci.* **2008**, *33* (2), 167–179.
(7) Sanabria-DeLong, N.; Crosby, A. J.; Tew, G. N. Photo-Cross-Linked PLA-PEO-PLA Hydrogels from Self-Assembled Physical Networks: Mechanical Properties and Influence of Assumed Constitutive Relationships. *Biomacromolecules* **2008**, *9* (10), 2784–2791.
(8) Di Biase, M.; de Leonardis, P.; Castelletto, V.; Hamley, I. W.; Derby, B.; Tirelli, N. Photopolymerization of Pluronic F127 diacrylate: a colloid-templated polymerization. *Soft Matter* **2011**, *7*, 4928.
(9) Babu, S.; Gimel, J. C.; Nicolai, T. Phase separation and percolation of reversibly aggregating spheres with a square-well attraction potential. *J. Chem. Phys.* **2006**, *125*, 184512.
(10) Brown, W. *Light Scattering: Principles and Development*; Clarendon Press: Oxford, 1996.
(11) Nicolai, T. Food structure characterisation using scattering methods. In *Understanding and Controlling the Microstructure of Complex Foods*; McClements, D. J., Ed.; Woodhead: Cambridge, 2007; pp 288−310.
(12) Berne, B. J.; Pecora, R. *Dynamic Light Scattering*; Dover: Mineola, NY, 2000.
(13) Stepanek, P. In *Dynamic Light Scattering*; Brown, W., Ed.; Oxford University Press: Oxford, 1993.
(14) Jakes, J. *Collect. Czech. Chem. Commun.* **1995**, *60*, 2011.
(15) Kalyanasundaram, K.; Thomas, J. K. Environmental Effects on Vibronic Band Intensities in Pyrene Monomer Fluorescence and Their Application in Studies of Micellar Systems. *J. Am. Chem. Soc.* **1977**, *99* (7), 2039–2044.
(16) Wilhelm, M.; Zhao, C.-L.; Wang, Y.; Xu, R.; Winnik, M. A.; Mura, J.-L.; Riess, G.; Croucher, M. D. Poly(styrene-ethylene oxide) Block Copolymer Micelle Formation in Water: A Fluorescence Probe Study. *Macromolecules* **1991**, *24*, 1033–1040.
(17) Laflèche, F.; Durand, D.; Nicolai, T. Association of adhesive spheres formed by hydrophobically end-capped PEO. 1. Influence of the presence of single end-capped PEO. *Macromolecules* **2003**, *36* (4), 1331–1340.
(18) Piogé, S.; Fontaine, L.; Gaillard, C.; Nicol, E.; Pascual, S. Self-Assembling Properties of Well-Defined Poly(ethylene oxide)-b-Pol(ethyl acrylate) Diblock Copolymers. *Macromolecules* **2009**, *42*, 4262–4272.
(19) Babu, S.; Rottereau, M.; Nicolai, T.; Gimel, J. C.; Durand, D. Flocculation and aggregation in reversible cluster-cluster aggregation. *Eur. Phys. J. B* **2006**, *19*, 2003.
(20) Wessel, R.; Ball, R. C. Cluster-cluster aggregtaion with random bond breaking. *J. Phys. A: Math. Gen.* **1993**, *26*, L159–L163.
(21) Stauffer, D.; Aharony, A. *Introduction to Percolation Theory*, 2nd ed.; Taylor & Francis: London, 1992; p 181.
(22) Cohen, R. J.; Benedek, G. B. Equilibrium and kinetic theory of polymerization and the sol-gel transition. *J. Phys. Chem.* **1982**, *86* (19), 3696–3714.
(23) Indei, T.; Koga, T.; Tanaka, F. Theory of shear-thickening in transient networks of associating polymer. *Macromol. Rapid Commun.* **2005**, *26* (9), 701–706.